A simple experimental system to illustrate the nonlinear properties of a linear chain under compression

Weaire, Denis; Irannezhad, Ali; Mughal, Adil; Hutzler, Stefan

Published in:
American Journal of Physics

DOI:
10.1119/10.0000667

Publication date:
2020

Citation for published version (APA):
Weaire, D., Irannezhad, A., Mughal, A., & Hutzler, S. (2020). A simple experimental system to illustrate the nonlinear properties of a linear chain under compression. *American Journal of Physics* , *88*(5), 347-352. https://doi.org/10.1119/10.0000667

A simple experimental system to illustrate the nonlinear properties of a linear chain under compression

Denis Weaire,[1] Ali Irannezhad,[1] Adil Mughal,[2] and Stefan Hutzler[1,*]

[1] *School of Physics, Trinity College Dublin, Dublin 2, Ireland*

[2] *Department of Mathematics, Aberystwyth University, Penglais, Aberystwyth, Ceredigion, Wales SY23, United Kingdom*

(Dated: January 8, 2020)

Abstract

A linear chain of spheres confined by a transverse harmonic potential experiences localized buckling under compression. Here we present simple experiments using gas bubbles in a liquid-filled tube to demonstrate this phenomenon. Our findings are supported semi-quantitatively by numerical simulations. In particular we demonstrate the existence of a critical value of compression for the onset of buckling.

I. INTRODUCTION

Linear chains of particles have long been popular in providing simple examples for analysis using classical mechanics. Consequentially, numerous classroom demonstrations entail the study of such chains; examples include the problem of determining the force exerted by a falling chain[1–3] (a long-standing problem which continues to provoke debate[4]) the vibrations (and normal modes[5]) of a chain of particles[6], as a means of demonstrating the properties of the catenary[7] (and related curves), the physics of collisions and shock waves[8], as well as numerous other interesting problems suitable for the undergraduate physics curriculum[9].

Much of this work has been largely confined to linear elastic theory and dynamics[5,10].The pedagogical value of such models lies in their essentially one-dimensional nature which is helpful for observation, analysis and theory. In many respects they share the properties of two- and three-dimensional systems and therefore provide an easy introduction to these.

Here we extend the suite of classroom demonstrations to linear chains of mutually repelling particles. The particles are compressed along the length of the chain (corresponding to being trapped by an axial potential in the related physical systems mentioned below) while also being confined in the radial (or transverse) direction by a cylindrically symmetric potential. We will focus on the case of static equilibrium, for compressions large enough to induce complex nonlinear properties.

Our demonstration experiments and the accompanying theory and simulations make contact with ongoing research in a number of areas, where they may serve as illustration of the underlying physics, but can also offer inspiration for further measurements. Relevant research includes that on laser-cooled ions in Penning traps[11] and dusty plasmas[12]. Related structures have also been observed in experiments with colloids[13], microfluidic crystals[14] and magnetic particles[15]. A more accessible system was introduced by[16], using buoyant plastic spheres in a water-filled tube, rotated by a lathe; structures for a wide range of compression were reported, and were further analyzed theoretically in[17].

The type of arrangement formed by the particles depends on the competition between radial and axial confinement. When radial confinement dominates the particles form a straight linear chain; however, on reducing the radial force the preferred (minimum energy) state of the system transitions from a linear chain to a modulated zigzag structure[18]. Such systems have many interesting properties, including buckling, localization (sometimes described in

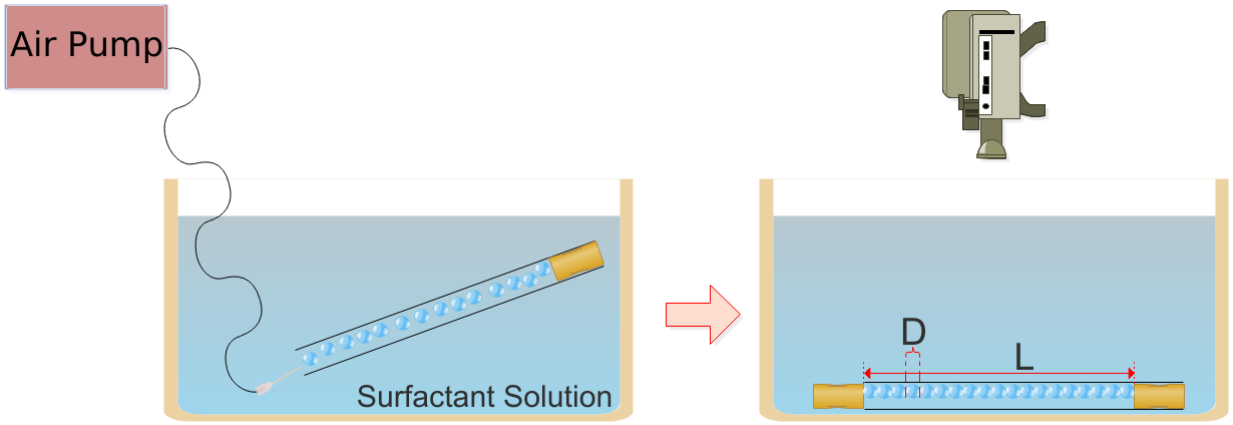

FIG. 1: Sketch of the experimental set-up and procedure. After filling, the tube is tilted to release any excess bubbles, so that only a single line of bubbles remains. The second stopper is then inserted and manually adjusted to vary the axial compression of the bubble chain. The observation is carried out under water to avoid air entering the tube. (Inner diameter of the tube: 6.7 mm, outer diameter 8.0 mm, axial extension of bubbles: $D = 2.3$ mm)

terms of "kinks" or "solitons"), a variety of alternative (meta)stable structures, topological changes, bifurcation diagrams, and a Peierls-Nabarro potential for transitions between them[18,19]. The buckling of a linear chain has also been found relevant to mechanical properties of engineered materials[20] and to active colloidal chains in biology[21]. As mentioned, buckled structures commonly occur in formations of cooled ions in traps; these in turn find a range of advanced applications in spectroscopy, quantum computing and reaction kinematics (see[22] for a recent review).

In the present paper we describe for the first time a very simple experimental set-up that may be used to demonstrate and measure many of the generic nonlinear properties of such a system. It is easily realized with the simplest equipment available in the class-room (test tube with stoppers, aquarium pump, dish-washing solution)(Fig.1). The experimental arrangement consists of gas bubbles trapped in a horizontal liquid-filled tube. The bubbles are confined axially by opposing walls (stoppers) at either end of the tube. Compressing the linear chain of bubbles leads to buckling. Further increase of compression generates a sequence of different modulated zigzag structures. These relate also to previous studies of

the packings of hard spheres in cylinders[23].

This new type of experiment will enable many fine details to be explored, which have not so far been analysed for any of the more sophisticated systems mentioned above, especially when combined with the numerical simulations of the kind presented here.

II. EXPERIMENTAL METHOD AND RESULTS

Bubbles of equal size are produced by blowing air through a nozzle into a solution of commercial detergent (*"Fairy Liquid"*) using an air pump with a flow control valve. The bubbles are introduced into a perspex tube (inner diameter 6.7 mm, outer diameter 8 mm) which is placed horizontally at the bottom of the container filled with the surfactant solution (Fig.1), and stoppers are inserted. For a certain separation L_0 of these stoppers N bubbles are only just in contact with one another and the two stoppers. The uncompressed axial extension D of the bubbles is then $D = L_0/N$. In the experiments reported below we have used $N = 19$ bubbles with $D = 2.3$ mm.

Decreasing the length of confinement L by manually pushing the stoppers, we may observe and record (as photos or videos) the structures that are formed; for an example see figure 2. For small values of compression Δ, defined as $\Delta = N - L/D$, the chain of bubbles remains straight, with all bubbles suffering equal deformation. However, at some critical value of compression Δ, buckling occurs (see figure 2). The critical value of Δ is *zero* for hard spheres, and finite for soft (elastic) spheres, as in the case of bubbles.

In this regime the buckled structures are found to be *planar* for rotating cylinders[16,17]. They are *approximately* so for the technique here introduced. Further examples are shown in figure 3 and numbered for later reference.

To characterize these structures under compression in a simple way we have determined the width W of the minimal rectangular box which contains all the bubbles of a particular chain; for an example see figure 4 (top). This is a convenient parameter for measurement by hand from photographs. However, the data reported below was obtained using the image processing software *ImageJ*[24].

Figure 4 shows the rescaled width W/D for ten different values of compression Δ, for all the structures shown in Figure 3. The width increases strongly once the compression exceeds its critical value.

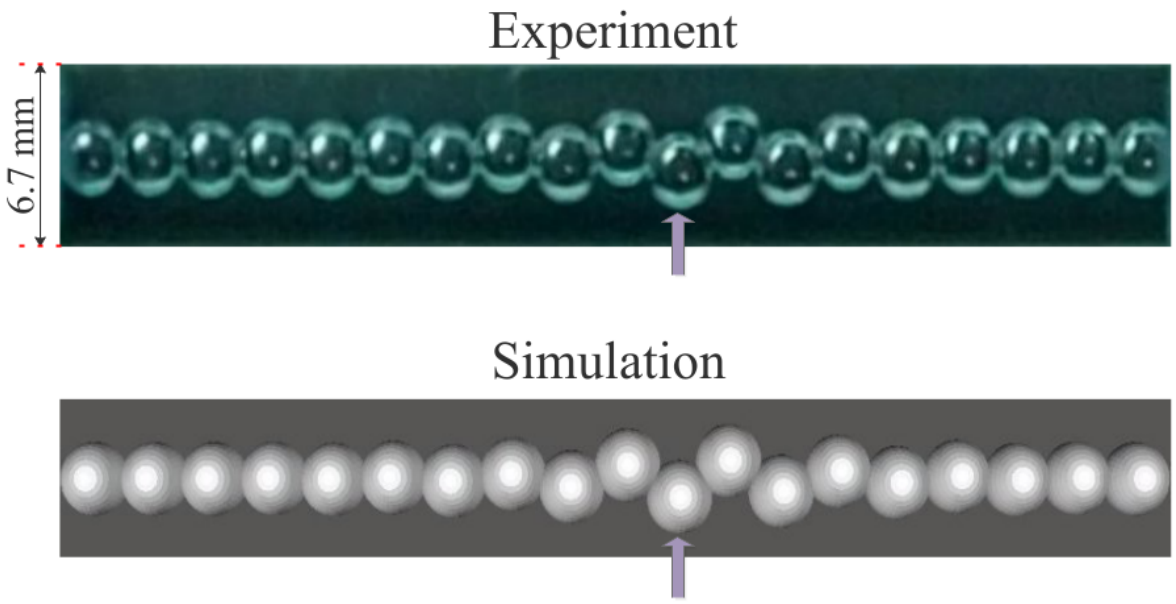

FIG. 2: The compression of a linear chain of bubbles results in buckling, once a critical value of compression is exceeded. (a) Photograph of 19 gas bubbles in a tube filled with surfactant solution for compression $\Delta = 2.36$ (corresponding to image/datapoint 6 in figures 3 and 4). (b) A computer simulation of 19 soft spheres using the model of section III and ratio of force constants $k = 2.25$ yields a closely similar structure, cf. the region around the maximally displaced bubble, marked by an arrow.

Before describing the data in detail we will comment on a particular feature of the experimental set-up. In the case of an uncompressed chain ($\Delta = 0$) of *hard* spheres the width W is simply D (which in this case coincides with the sphere diameter). However, two effects play a role when interpreting W in our experiments with bubbles. Firstly, optical distortion arising from using liquid-filled tubes leads to a small increase in the ratio W/D also in the case of hard spheres for these experiments. (We found $W/D \simeq 1.04$ for a chain of *hard* plastic spheres of diameter 3 mm, placed in the water-filled tube within the container used for the bubble experiments.) Secondly, our gas bubbles are not spherical even under zero compression Δ, due to the effect of buoyancy, pressing them against the tube surface.

The combination of these two effects can account for the value of $W/D \simeq 1.14$ found for small compression, $\Delta \simeq 0.13$, see Figure 4. Upon further compression the width increases slightly to about $W/D \simeq 1.23$ for $\Delta \simeq 1.56$. At $\Delta = 2.13$ the chain has clearly buckled,

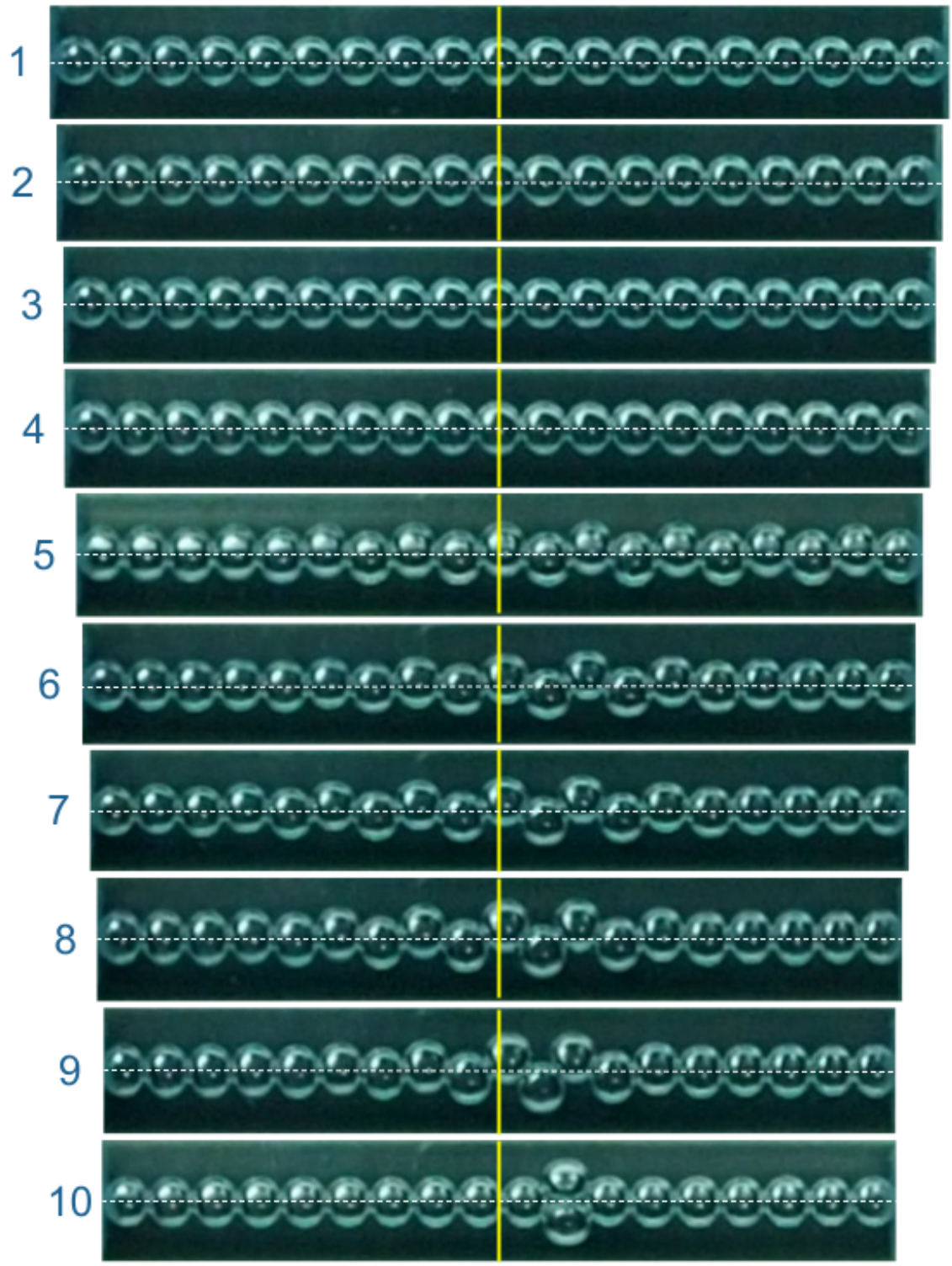

FIG. 3: Sequence of 10 photographs of a chain of 19 bubbles under compression ($\Delta_i = 0.13, 0.32, 1.00, 1.56, 2.13, 2.36, 2.56, 2.62, 2.80, 2.85$). For geometrical dimensions see text. Compression was progressively increased by small amounts. The solid yellow line marks the centre of each chain. Buckling becomes visible at the fifth image, leading to a modulated zig-zag pattern of bubble displacement. Note the eventual exceptional case 10, in which a transverse pair (or *doublet*) of bubbles is surrounded by a straight linear chain. Variation of experimental procedure can produce localization at other places in the chain.

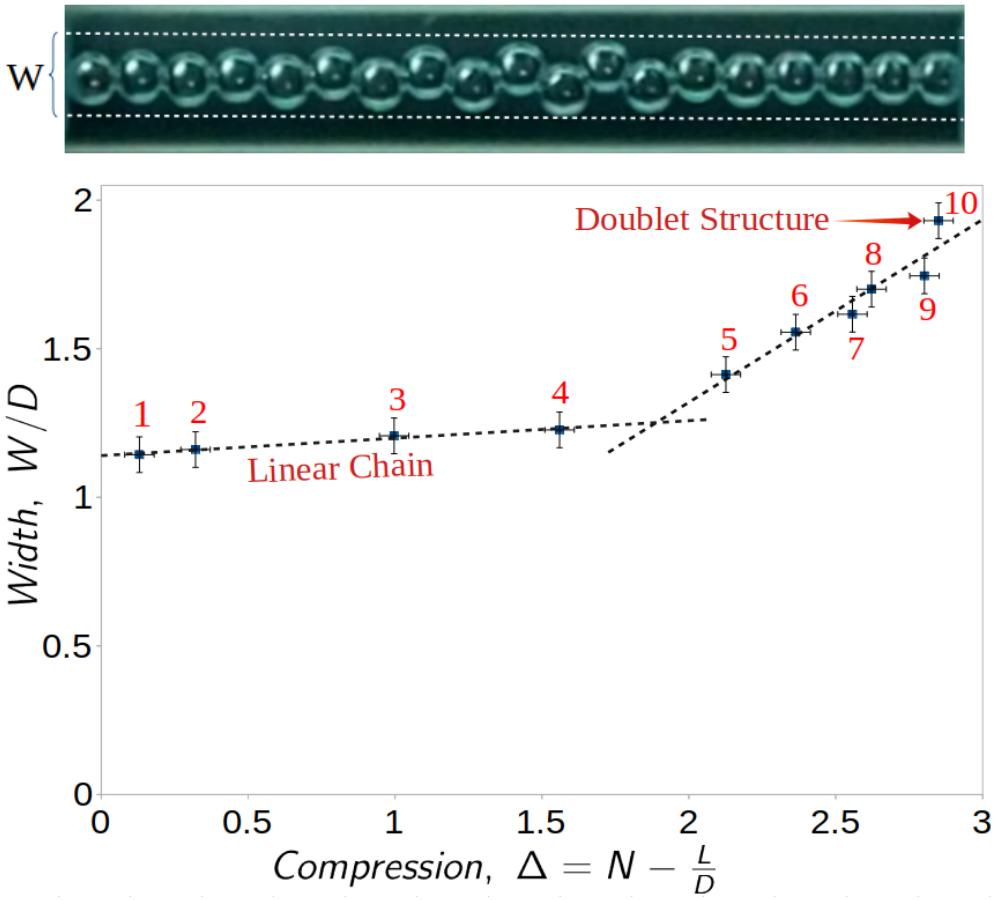

FIG. 4: The variation of the normalized chain width W/D with compression Δ reveals the onset of buckling at a critical value $\Delta_c \simeq 1.9$. Values of Δ exceeding 2.7 lead to the occurrence of an increasing number of doublets within the same structure. (Numbers refer to the chains shown in figure 3, the photograph at the top marks the width W for structure 7.)

causing a large increase in width to about $W/D \simeq 1.41$. A further increase in compression results in a roughly linear increase of W, as the profile of lateral displacement becomes increasingly *localized* (see photograph in figure 4).

At values of compression exceeding $\Delta \simeq 2.7$ the localized zig-zag structure gives way to a straight chain containing a 'doublet', a transverse pair of bubbles.

A linear extrapolation of the width variation of the buckled structures would identify the onset of buckling at around $\Delta_c \simeq 1.75$. However, buckling is generally associated with a square-root scaling in compression, visible in the simulations described in section III. Taking

this into account we estimate the critical value of compression to lie somewhere in the range $1.8 < \Delta_c < 2.0$ (figure 4).

III. THEORY AND SIMULATIONS

We have made a preliminary comparison of the above data with results from an elementary numerical simulation. The basis for this is explained below. We should emphasize that the simple model for bubble-bubble interactions which we will employ is *not* intended to be accurate, so comparison will not be fully quantitative.

We will be concerned with structures of length L, made up of N idealized spherical particles of diameter D; see figure 5. We will restrict our analysis to structures formed under low compression, $\Delta = N - L/D$. We have already shown one simulation result in figure 2.

To obtain such numerical results we have used the Durian Model[25,26]. This represents bubbles as spheres whose overlap is associated with a repulsive force between the bubble centres. (A similar approach was suggested earlier[27].) For a pair of bubbles of equal size, the interaction energy E_i is $E_i = \frac{k_1}{2}\left(|\vec{R}_i - \vec{R_{i+1}}| - D\right)^2$, where $\vec{R}_i$ are sphere centres and k_1 is the spring constant for bubble-bubble interaction. The crude model has proved useful in foam physics[28,29] in providing qualitative and semi-quantitative insights.

In the present case we write the total energy due to *contacts*, including the contribution of the two bubbles in contact with the confining walls ($i = 1$ and ($i = N$), in the approximate form

$$E_{contact} = \frac{k_1}{2}\left[\sum_{i=1}^{N-1}\left(\left(X_i - X_{i+1}\right)^2 + \left(Y_i - Y_{i+1}\right)^2\right)^{1/2} - D\right)^2 + \left(\frac{D}{2} - X_1\right)^2 + \left(\frac{D}{2} + X_N - L\right)^2\right]. \tag{1}$$

Only the coordinates X_i and Y_i enter, an approximation that makes the system planar and is valid for small values of compression.

The corresponding approximation for the gravitational potential energy due to the *buoyancy* of a particle held in place by the cylindrical surface is

$$E_{gravity} = \frac{k_2}{2}\sum_{i=1}^{N} Y_i^2. \tag{2}$$

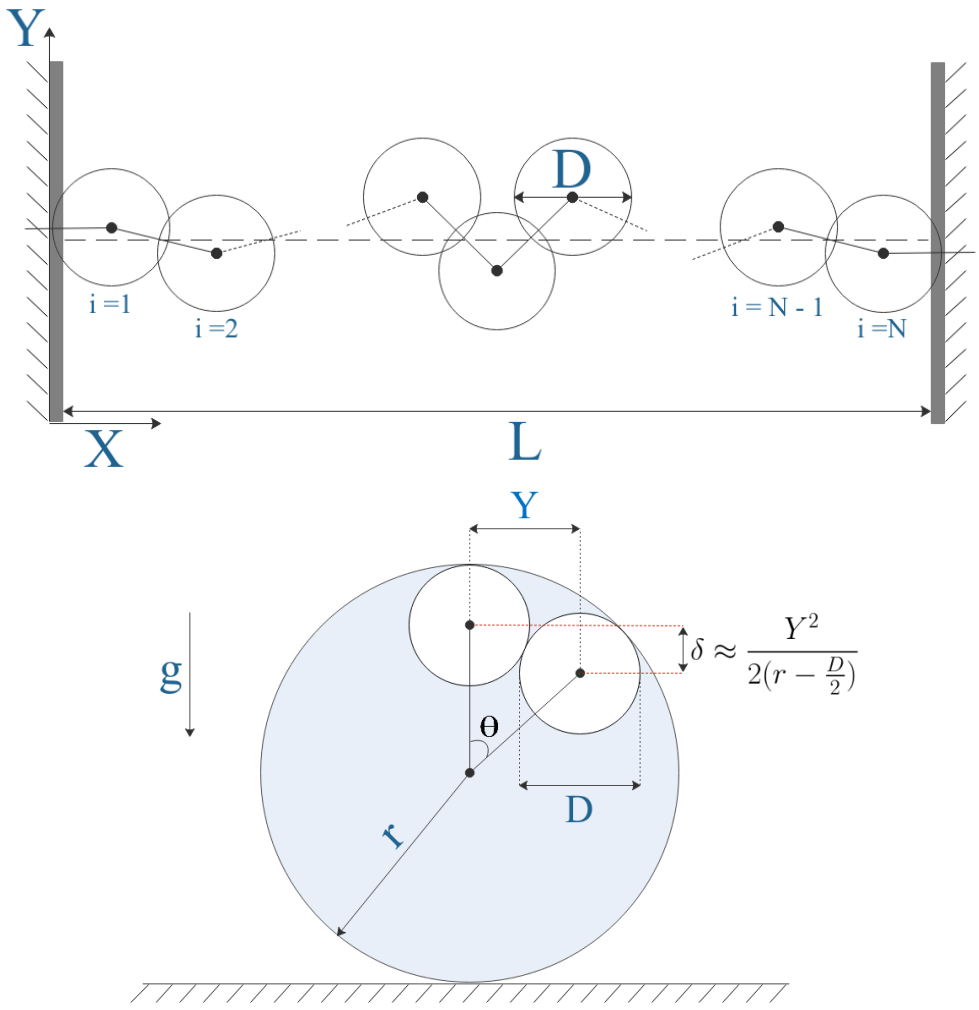

FIG. 5: Schematics for the modeling of a chain of soft spheres under compression. (a) Top view and notation. (b) View along the X direction, showing bubbles (diameter D) pressed against the surface of a liquid filled tube (radius r). For small displacements Y of a bubble in the horizontal direction its downward movement leads to an increase in potential energy due to buoyancy of approximately $\frac{1}{2}\frac{\Delta\rho g V}{(r-D/2)}Y^2$. Here $\Delta\rho$ is the density difference and V is the volume of the bubble, $V = \frac{4}{3}(\frac{D}{2})^3\pi$.

The force constant k_2 is given by

$$k_2 = \Delta\rho g[\frac{4}{3}(\frac{D}{2})^3\pi]/(r - D/2), \tag{3}$$

where $\Delta\rho$ is the density difference of gas and liquid, g is acceleration due to gravity and r is the radius of the cylinder, see figure 5 (b).

The total energy is thus approximated by $E_{total} = E_{contact} + E_{gravity}$. Expressed as a

dimensionless energy, $E = E_{total}/(k_2 D^2)$, this may be written as

$$E(\Delta) = \frac{1}{2}k\sum_{i=0}^{N}\left(\delta_{i,i+1}-1\right)^2 + \frac{1}{2}\sum_{i=1}^{N} y_i^2, \tag{4}$$

where we have introduced the dimensionless quantities $x_i = X_i/D$, $y_i = Y_i/D$, $\delta_{i,i+1} = ((x_i - x_{i+1})^2 + (y_i - y_{i+1})^2)^{1/2}$ (for $0 < i < N$), $\delta_{0,1} = \frac{3}{2} - x_1$, $\delta_{N,N+1} = \frac{3}{2} + x_n - (N - \Delta)$, and the ratio of the two force constants

$$k = k_1/k_2. \tag{5}$$

This is essentially the same expression used by[20].

The system has been reduced to two dimensions. The situation is rather different in the other physical systems to which we referred in section I, where planar structures are found to arise for only low compressions, but are not imposed by geometry at the outset (as we have done here). That is, planar structures are found in practice and become twisted at higher compression.

Starting from a small value of compression Δ, and a straight linear chain, we progressively increase Δ. For each step the previous equilibrium structure is used as the starting structure for minimization (in accord with the experimental procedure). Energy E, eqn.(4), is minimized numerically with respect to the cordinates x_i and y_i.

Below a critical value of compression (which depends on the value for the ratio k of the force constant, eqn.(5)) the minimum energy arrangement corresponds to that of a straight linear chain, but this buckles to form a zig-zag chain at a critical value of compression, as in the experiment. (A small perturbation is necessary to promote the instability.)

We performed computations for increments of $\delta\Delta = 0.01$ up to compression $\Delta = 3.0$ for various values of k. Results for $k = 2.5$ and $N = 19$ are collated in Fig.6, in terms of the dimensionless maximum transverse displacement, $y_{max} = \max(|y_i|)$. We have found this to be a more straightforward quantity for comparison with experiment, rather than width W, since W is affected by both optical distortion and bubble deformation, as discussed above.

For values of compression slightly exceeding $\Delta_c = 1.83$ we find y_{max} to vary as $(\Delta - \Delta_c)^{1/2}$, as is generally the case in buckling transitions. In this range the envelope of the displacement profile is broad (roughly of cosine form).

For higher values of Δ there is increased localization of buckling, as in the example shown in Fig.2. Finally, there is a sudden jump in the maximum transverse displacement

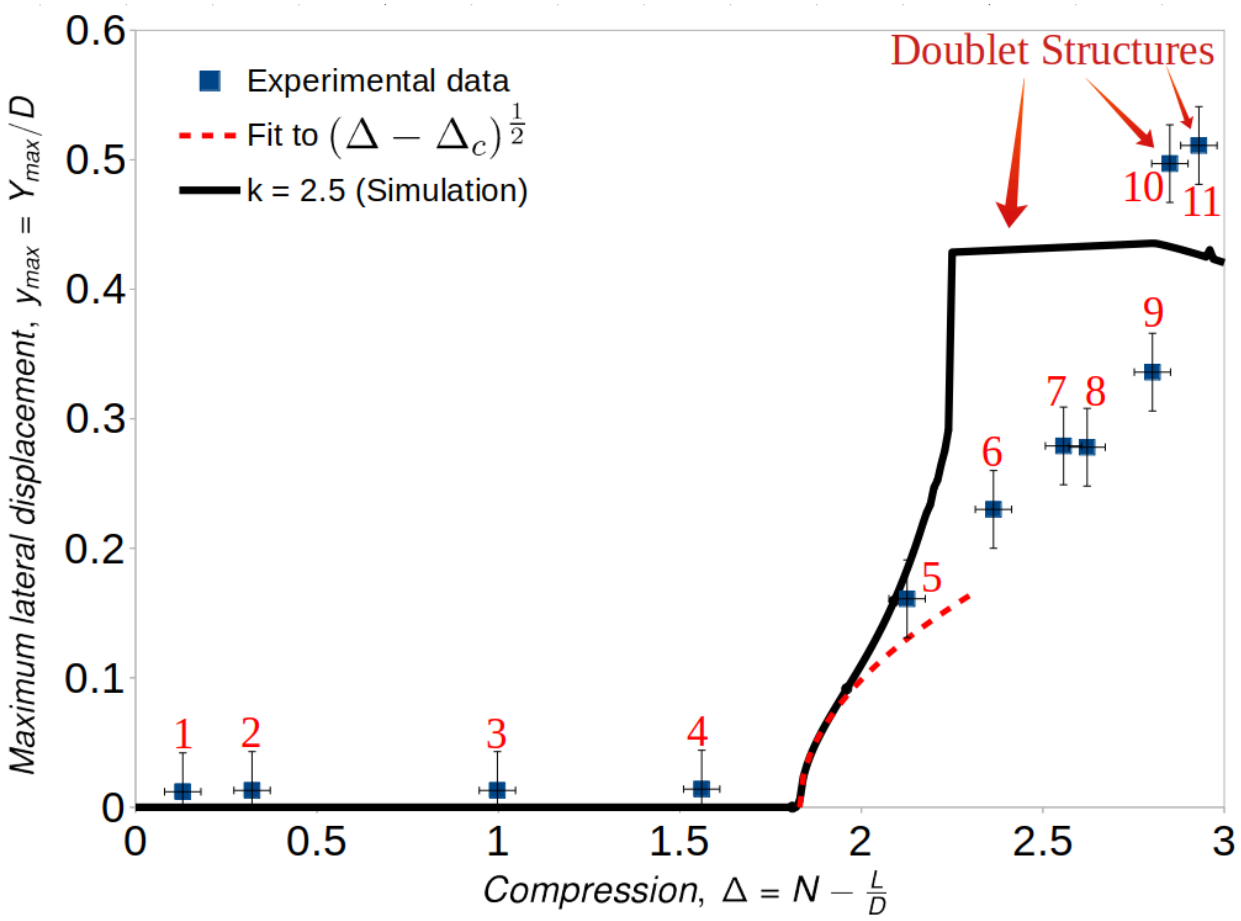

FIG. 6: Variation of maximum lateral bubble displacement y_{max} with compression Δ. Data points correspond to the experimental data of figure 4. The solid line represents numerical data obtained from a minimization of the energy of a chain of soft particles, eqn.(4), for a value of the force constant ratio $k = 2.5$. At the onset of buckling the numerical results indicate a square-root dependence of y_{max} with compression.

with increasing compression; at this point the doublet structure (with a transverse pair of spheres) becomes favourable. The maximum transverse displacement associated with this increases very slightly with compression, before encountering a further transition. Full details of this rich scenario, as well as a comprehensive overview of theory and simulation, are reserved for a future paper.

IV. COMPARISON WITH EXPERIMENT

Fig.6 also presents experimental data for comparison. Here the maximum lateral bubble displacement $y_{max} = Y_{max}/D$ was obtained by first determining the lateral midpoint of each bubble and then measuring its distance to the tube axis, using the photographs in Fig. 3. (The representation of the buckling of a bubble chain using its width W, as in figure 4, might be more suited in the context of a class-room, since it requires less measurements.)

There is broad agreement between experiment and theory for $k = 2.5$. Increasing k moves the critical value of compression Δ_c towards zero, the value found for the case of hard spheres ($k_1 \to \infty$)[17]. The theory also correctly predicts the occurrence of a doublet structure (number 10 in Fig.3).

We may also seek to estimate k from the relevant experimental parameters. Setting the dimensional spring constant $k_1 = \gamma/2$[26], where $\gamma \simeq 0.03\ N/m$ is the surface tension of our surfactant solution, we can evaluate $k = k_1/k_2$ using eqn.(3). Inserting $\rho = 1000\ kg/m^3$, $D = 2.3\ mm$ and $r = 3.35\ mm$, we obtain $k \simeq 0.5$, i.e. a value of the same order of magnitude as the one found from comparison with numerical data (figure 6).

V. FURTHER DEMONSTRATION EXPERIMENTS

The effects of buckling in a chain of particles can also be illustrated using even simpler experimental set-ups.

Figure 7 shows an example of a buckled chain of 30 steel spheres (ball bearings) in a tube, closed with two stoppers. In order to reduce friction we immersed the spheres in vegetable oil. Related structures can also be investigated using golf or tennis balls in a perspex tube, or even in a section of roof gutter, and doubtless other ingredients await discovery and exploitation.

VI. SUMMARY AND OUTLOOK

We have described a simple experimental set-up, suitable for the class- or lecture room, for the exploration of the nonlinear properties of a chain of spheres under compression. The experiment demonstrates these properties which have recently lead to a number of publications on nano-scale systems[11,12,30]. The simulation method described is straightforward,

FIG. 7: Buckled chain of 30 steel spheres (diameter 6.32 mm) confined in a perspex cylinder (inner cylinder diameter 1.6 cm) and under compression, $\Delta = 0.85$. The spheres, which are undeformed, are immersed in vegetable oil to reduce friction between them. (The presence of the oil leads to a large optical distortion; the measured ratio of lateral sphere extension to sphere diameter is about 1.9.)

and reproduces key features of the experiment. It might also lend itself to exploration in the context of a computational physics laboratory.

The use of bubbles offers an additional dimension to the experiment which could be explored: the effective softness of the bubbles is a function of their size. In the present preliminary work we have used only a single bubble size and treat the softness parameter (constant k in equation 4) as adjustable. Note that k can also be varied by varying the cylinder radius.

In previous work we analysed the desk-top toy called "Newton's Cradle", i.e. a linear chain of contacting metal balls, suspended from a railing by attached strings, and thus subject to a harmonic confining potential, albeit in the direction of the chain[31]. As is the case in the present work, this system proved remarkably rich when analyzed in detail. In particular the break-up of the line of balls following the initial impact is generally overlooked in physics textbook descriptions. It is hoped that the bubble chain experiment presented here, which shares with the cradle an economy of effort and expense, provides similar stimulation for students to look for non-trivial phenomena in chains of confined spheres.

ACKNOWLEDGMENTS

This work was supported by EPSRC grants EP/K032208/1 and EP/R014604/1, and Science Foundation Ireland (SFI) grant 13/IA/1926. AI acknowledges funding from the

TCD Provost's PhD Project Awards.

---

* permanent address: School of Physics, Trinity College Dublin, Dublin 2, Ireland; stefan.hutzler@tcd.ie

[1] MG Calkin and RH March. The dynamics of a falling chain: I. *American Journal of Physics*, 57.2, 154-157, 1989.

[2] E Hamm and JC Géminard. The weight of a falling chain, revisited. *American Journal of Physics*, 78.8, 828-833, 2010.

[3] JC Géminard and L Vanel. The motion of a freely falling chain tip: Force measurements. *American Journal of Physics*, 76.6, 6541-545, 2008.

[4] AA Domnyshev, VA Kalinichenko and PM Shkapov. On two experiments with falling chains. *Journal of Physics: Conference Series*, Vol. 1301. No. 1. IOP Publishing, 2019.

[5] JD Louck. Exact normal modes of oscillation of a linear chain of identical particles. *American Journal of Physics*, 30, 585, 1962.

[6] D Oliver. Oscillation of a paper-clip chain. *The Physics Teacher*, 34, 446-447, 1996.

[7] F Behroozi, P Mohazzabi and JP McCrickard. Remarkable shapes of a catenary under the effect of gravity and surface tension. *Journal of Physics*, 62.12, 1121-1128, 1994.

[8] F Herrmann and M Seitz. How does the ballchain work?. *American Journal of Physics*, 50.11, 977-981, 1982.

[9] G Péter, G Honyek and KF Riley. 200 puzzling physics problems: with hints and solutions. *Cambridge University Press*, 2001.

[10] M Reinsch. Dispersionfree linear chains. *American Journal of Physics*, 62, 271, 1994.

[11] RC Thompson. Ion coulomb crystals. *Contemporary Physics*, 56(1):63–79, 2015.

[12] A Melzer. Zigzag transition of finite dust clusters. *Physical Review E*, 73(5):056404, 2006.

[13] AV Straube, AA Louis, J Baumgartl, C Bechinger, and RPA Dullens. Pattern formation in colloidal explosions. *EPL (Europhysics Letters)*, 94(4):48008, 2011.

[14] T Beatus, T Tlusty, and R Bar-Ziv. Phonons in a one-dimensional microfluidic crystal. *Nature Physics*, 2(11):743, 2006.

[15] JE Galván-Moya, D Lucena, WP Ferreira, and FM Peeters. Magnetic particles confined in a modulated channel: Structural transitions tunable by tilting a magnetic field. *Physical Review*

E, 89(3):032309, 2014.

[16] T Lee, K Gizynski, and BA Grzybowski. Non-equilibrium self-assembly of monocomponent and multicomponent tubular structures in rotating fluids. *Advanced Materials*, 29(47):1704274, 2017.

[17] J Winkelmann, A Mughal, D Weaire, and S Hutzler. Equilibrium configurations of hard spheres in a cylindrical harmonic potential. *EPL (Europhysics Letters)*, 127:44002, 2019.

[18] H Landa, B Reznik, J Brox, M Mielenz, and T Schätz. Structure, dynamics and bifurcations of discrete solitons in trapped ion crystals. *New Journal of Physics*, 15(9):093003, 2013.

[19] M Mielenz, J Brox, S Kahra, G Leschhorn, M Albert, T Schätz, H Landa, and B Reznik. Trapping of topological-structural defects in coulomb crystals. *Physical Review Letters*, 110(13):133004, 2013.

[20] RK Pal, F Bonetto, L Dieci, and M Ruzzene. A study of deformation localization in nonlinear elastic square lattices under compression. *Philosophical Transactions of the Royal Society A: Mathematical, Physical and Engineering Sciences*, 376(2127):20170140, 2018.

[21] S Gonzalez and R Soto. Active colloidal chains with cilia-and flagella-like motion. *New Journal of Physics*, 20(5):053014, 2018.

[22] BR Heazlewood. Cold ion chemistry within coulomb crystals. *Molecular Physics*, pages 1–8, 2019.

[23] A Mughal, HK Chan, D Weaire, and S Hutzler. Dense packings of spheres in cylinders: Simulations. *Physical Review E*, 85(5):051305, 2012.

[24] MD Abràmoff, PJ Magalhães, and SJ Ram. Image processing with ImageJ. *Biophotonics international*, 11(7):36–42, 2004.

[25] DJ Durian. Foam mechanics at the bubble scale. *Phys. Rev. Lett.*, 75:4780–4783, 1995.

[26] DJ Durian. Bubble-scale model of foam mechanics: Melting, nonlinear behavior, and avalanches. *Phys. Rev. E*, 55:1739–1751, 1997.

[27] F Bolton and D. Weaire. Rigidity loss transition in a disordered 2D froth. *Physical Review Letters*, 65:3449, 1990.

[28] D. Weaire and S. Hutzler. *The physics of foams*. Clarendon press, Oxford, 1999.

[29] I Cantat, S Cohen-Addad, F Elias, F Graner, R Höhler, O Pitois, F Rouyer, and A Saint-Jalmes. *Foams: structure and dynamics*. Oxford University Press, 2013.

[30] AV Chaplik. Instability of quasi-one-dimensional electron chain and the string-zigzag structural transition. *JETP Lett*, 31(5):275–278, 1980.

[31] S Hutzler, G Delaney, D Weaire, and F MacLeod. Rocking Newton's Cradle. *American Journal of Physics*, 72(12):1508–1516, 2004.